



## EXPERIMENTAL AND NUMERICAL ANALYSIS OF STEEL FIBER REINFORCED CONCRETE PAVEMENT

Dr. Zainab A. AL-Kaissi<sup>1</sup>, Dr. Ahmed Saheb Daib<sup>2</sup>, \*Rusul Raed Abdull-Hussain<sup>3</sup>

- 1) Assist Prof., Highway and Transportation Engineering Department, Al-Mustansiriyah University, Baghdad, Iraq.
- 2) Assist Prof., Highway and Transportation Engineering Department, Al-Mustansiriyah University, Baghdad, Iraq.
- 3) M.Sc. Student, Highway and Transportation Engineering Department, Al-Mustansiriyah University, Baghdad, Iraq.

**Abstract:** The objective of this work is to compare the results obtained by modelling flexural strength test (Three Point Bending Test) of steel fiber reinforced concrete (SFRC) beam specimens using a numerical 3D modelling introduced by the computer code "ABAQUS" after conducting the (SFRC) beam specimens of (0.0, 0.4 and 0.8) % volume fraction of steel fiber ( $v_f$ ) to three point bending test using a hydraulically increasing universal testing machine under monotonic loads up to ultimate load with two different rates of loading (0.5 and 1) kN/sec. Deflection, stress and strain were obtained and the test is simulated using the computer code "ABAQUS". Test results show that deflection, stress and strain magnitudes are directly proportion to the increment of steel fiber and a good agreement can be seen between the experimental results and the analytical approaches, finally a comparison using "ABAQUS" is carried out between horizontal tensile stress and strain at bottom of concrete pavement for (0.0, 0.4, and 0.8) % ( $v_f$ ) of steel fiber and results analysis show that the ability of concrete pavement to withstand higher magnitudes of tensile stress and strain without deterioration increase as steel fiber content increase due to high tensile strength of steel fiber.

**Keywords:** Steel fiber reinforced concrete (SFRC), 3D modelling, Three point bending test, Deflection

### فحص ونمذجة التبليط الجاسيء المسلح بألياف الحديد

**الخلاصة:** الهدف من هذا البحث هو لمقارنة النتائج التي تم الحصول عليها عن طريق نمذجة اختبار قوة الأنحاء (اختبار الانحناء الثلاثي الساكن) للخرسانة المسلحة بألياف الحديد (SFRC) لنماذج العتبات باستخدام النمذجة العددية (3D) بواسطة شفرة الكمبيوتر "ABAQUS" بعد إجراء فحص الانحناء الثلاثي الساكن لنماذج العتبات (SFRC) المحتوية على (0.0، 0.4، و 0.8) % نسبة حجمية ( $v_f$ ) من الياف الحديد باستخدام الآلة العالمية لزيادة الحمل هيدروليكيًا (نظام MFL) بصورة ثابتة حتى التحميل النهائي مع معدلين مختلفين للتحميل (0.5 و 1) كيلو نيوتن / ثانية. تم الحصول على قيم كل من الهطول، الإجهاد والانفعال وتمت محاكاة الفحص باستخدام شفرة الكمبيوتر "ABAQUS". تظهر نتائج الاختبار أن قيم كلا من الهطول، الإجهاد والانفعال تتناسب طرديًا مع زيادة الياف الحديد وهناك تطابق جيد يمكن أن ينظر إليه بين النتائج العملية والمناهج التحليلية، وأخيرًا تمت مقارنة قيم إجهاد وانفعال الشد الأفقي باستخدام "ABAQUS" في الجزء السفلي من الرصف الخرساني للنسب الحجمية (0.0، 0.4، و 0.8) % ( $v_f$ ) من الياف الحديد والتي تبين من تحليل النتائج أن قدرة الرصف الخرساني على تحمل درجات أعلى من إجهاد الشد والانفعال دون حصول تدهور؛ تزداد مع زيادة محتوى ألياف الحديد بسبب قوة الشد العالية لألياف الحديد

\*Corresponding Author [Rusulabdhussain@yahoo.com](mailto:Rusulabdhussain@yahoo.com)

## 1. Introduction

Steel fiber reinforced concrete (SFRC) is concrete mixture made of Portland cement, fine aggregate, coarse aggregate and steel fibers. SFRC fails in tension when the discrete steel fibers break or pulled out of the matrix. Properties of SFRC are a computation of fiber properties, concrete properties and the properties of the interface between them. [1]

SFRC applications are diverse such in pavements, overlays, and shotcrete linings and such applications where the existence of continuous reinforcements is not necessary to the safety and integrity of the structure, the enhancements in flexural strength related with the fibers can be used to reduce thickness or improve performance of the sections, or both. Following are some of structural and nonstructural uses of SFRC: [2]

- Airport and highway paving and overlays: Particularly where a thinner than normal slab thickness is preferred.
- Industrial floors: For impact resistance and resistance to thermal shockwave.
- Refractory concrete: Using high-alumina cement in both castable and shotcrete uses.
- Bridge decks: As an overlay or topping where the major structural support is provided by an underlying reinforced concrete deck.
- In shotcrete linings: For underground support in mines and tunnels, usually with rock bolts.
- In shotcrete coverings: To stabilize soil slopes or aboveground rock, e.g., highway and railway embankments and cuts.
- Thin shell constructions: Shotcreted “foam domes”.
- Explosion-resistant structures: Commonly in combination with reinforcing bars.
- A possible future application in seismic-resistant structure.

Abaqus is a set of powerful engineering simulation programs, founded on the finite element method (FEM) that can solve problems ranging from relatively simple linear analyses to the most challenging nonlinear simulations. Abaqus offers a wide range of abilities for simulation of linear and nonlinear applications. Problems with multiple components are modeled by associating the geometry defining each component with the appropriate material models and specifying component interactions. In a nonlinear analysis Abaqus automatically chooses appropriate load increments and convergence tolerances and continually corrects them during the analysis to guarantee that an accurate solution is obtained efficiently. [3]

## 2. Material Characteristics

### 2.1. Cement

Ordinary Portland cement (type I) of Tasluja Factory is used in the present paper. Tables (1) and (2) show the chemical composition and physical properties of the cement used. This cement is tested and checked according to Iraqi Standard Specification.

Table 1. Chemical Composition of Cement\*

Compound Composition	Chemical Composition	Percentage by Weight	IQS 5:1984 Limits
Lime	CaO	62.22	-
Silica	SiO <sub>2</sub>	22.1	-
Alumina	Al <sub>2</sub> O <sub>3</sub>	5.49	-
Iron Oxide	Fe <sub>2</sub> O <sub>3</sub>	3.53	-
Magnesia	MgO	2.24	≤5
Sulfate	SO <sub>3</sub>	1.07	≤2.5
Loss on Ignition	L.O.I	0.09	≤4
Insoluble residue	I.R	0.32	≤1.5
Lime saturation factor	L.S.F	0.86	0.66-1.02
Main Compounds (Bogue's equation) percentage by weight of cement			
Tricalcium Silicate (C <sub>3</sub> S)		38.55	
Dicalcium Silicate (C <sub>2</sub> S)		33.15	
Tricalcium Aluminate (C <sub>3</sub> A)		8.58	
Tetracalcium Aluminoferrite (C <sub>4</sub> AF)		10.73	

\* All chemical tests were made by National Center for Construction Laboratories and Research (NCCLR).

Table 2. Physical Properties of Cement\*

Physical Properties	Test Result	IQS 5:1984 Limits
Fineness using Blain Air Permeability Apparatus (m <sup>2</sup> /kg)	310	250 min.
Soundness using Autoclave Method	0.19%	≤0.8
Setting Time using Vicat's Instruments		
Initial (min.)	165	45 min.
Final (hrs:min)	246	10 hrs. Max.
Compressive Strength for Cement Paste Cube (70.7 mm) at		
3 days (MPa)	16.4	15 min.
7 days (MPa)	27	23 min.
28 days (MPa)	35	additional

\* All physical tests were made by National Center for Construction Laboratories and Research (NCCLR).

## 2.2. Fine aggregate

Natural river sand from Al-Sudoor region is used. Table (3) and Table (4) shows the grading and physical properties of the fine aggregate respectively that are performed by the National Center for Construction Laboratories and Research (NCCLR).

## 2.3. Coarse aggregate

Crushed gravel brought from Al-Niba'ee region is used. The grading and physical properties of coarse aggregate shown in Tables (5) and (6) respectively. The mid-range of specification is used of aggregate gradation as plotted in Fig (1).

Table 3. Grading of Fine Aggregate AASHTO T-27-93.

No.	Sieve Size (mm)	% Passing by Weight	
		Selected Gradation of Aggregate %	AASHTO T-27-93
1	4.75	96	90-100
2	2.36	90	85-100
3	1.18	83	75-100
4	0.60	70	60-79
5	0.30	31	12-40
6	0.15	6.0	0-10

Table 4. Physical Properties of Fine Aggregate. \*

No.	Physical Properties	Test Results	Limits of Iraqi Specification SCRB,2003	Test No.
1	Specific Gravity	2.65	-	AASHTO T 84
2	Sulfate Content	0.08%	≤ 0.5%	
3	Absorption	0.75%	-	AASHTO T 84

\*All Test made by National Center for Construction Laboratories and Research (NCCLR).

Table 5. Grading of Coarse Aggregate.

Sieve Size (mm)	Coarse Aggregate Gradation	
	AASHTO M43, Size No. 67, (2003)	Selected Gradation of Aggregate
25	100	100
19	90-100	95
12	-	-
9.5	20-55	37.5
4.75	0-10	5
2.36	0-5	2.5

Table 6. Physical Properties of Coarse Aggregate\*.

No.	Physical Properties	Test Results	Limits of Specification	Test No.
1	Specific Gravity	2.6	--	AASHTO T- 85
2	Sulfate Content	0.087%	≤0.1%	AASHTO T-290
3	Absorption	0.63%	--	AASHTO T- 85
4	Percent of Passing no.200 by Weight	0.05%	≤1%	ASTM C 33/03
5	% Organic Impurities	0.2%	≤2%	ASTM C33/03

\*All Test made by National Center for Construction Laboratories and Research (NCCLR).

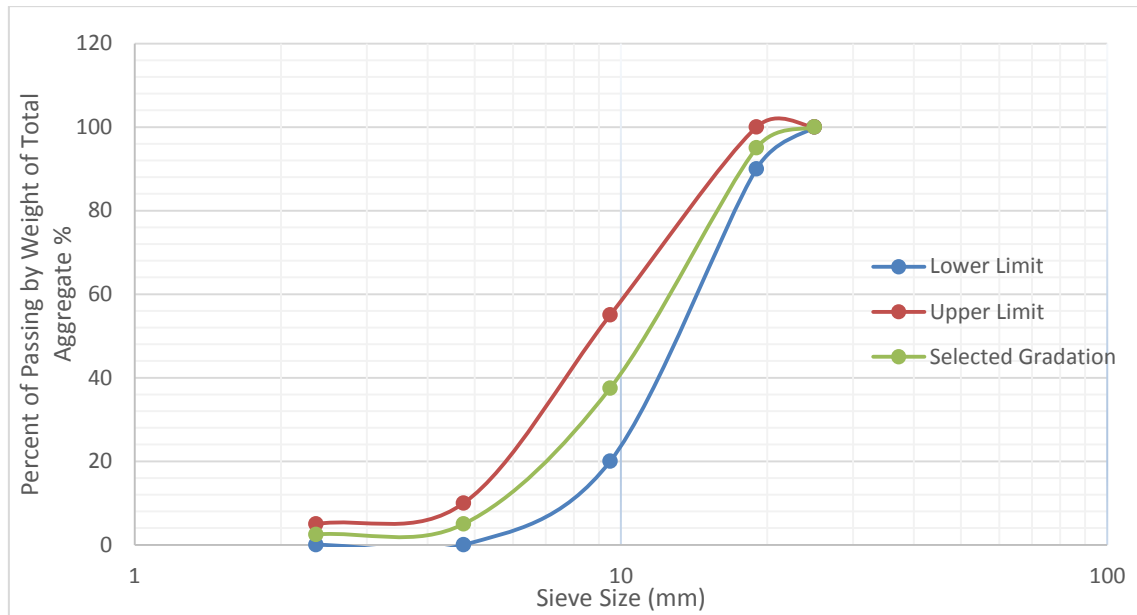


Figure 1. Specification Limits and Gradation of Coarse Aggregate.

### 2.4. Water

Potable water of Baghdad was used for casting and curing.

### 2.5. Steel Fiber

Dramix steel fibers manufactured by Bekaert Corporation were used at a (0.4) % and (0.8) % volume fraction % (*vf*) [4]. Table (7) gives properties of the steel fibers.

Table 7. Properties of steel fiber\*.

Commercial Name	Configuration	Property	Specifications
Dramix ZC 50/0.5	 Hooked Ends	Density	7860 kg/m <sup>3</sup>
		Ultimate Strength	1130 MPa
		Modulus of Elasticity	200x10 <sup>3</sup> MPa
		Strain at Proportion Limit	5650 x10 <sup>-6</sup>
		Poisson's Ratio	0.28
		Average Length	50 mm
		Nominal Diameter	0.5 mm
		Aspect Ratio ( $L_f/D_f$ )	100

\*Supplied by the manufacturer.

### 2.6. Fluidifying Additives

Sika ViscoCrete-5930, is a third generation of superplasticizers for concrete and mortar, was used. It meets the requirements for superplasticizers according to ASTM C 494 Types G and F and BS EN 934 Part 2: 2001. Main properties of the used superplasticizers shown in Table (8).

Table 8. The Properties of Fluidifying Additive\*.

Appearance	Turbid Liquid
Density	1.08 kg/l <sub>t</sub> _0.005
Basis	Aqueous solution of modified polycarboxylate
Packing	5 kg,20 kg,200 kg drums <ul style="list-style-type: none"> <li>• Strong self-compacting behavior</li> <li>• Extremely high water reduction</li> </ul>
Benefit	<ul style="list-style-type: none"> <li>• Excellent flow ability</li> <li>• Increase high early strengths development</li> <li>• Improve shrinkage and creep behavior</li> </ul>
Shelf life	Shelf life at least 12 months from date of production

\*Supplied by the manufacturer.

### 2.7. Concrete Proportions

A common concrete matrix was used in all mixes. The mixing proportion of (cement: sand: aggregate) was 1:2:2 by weight and the water–cement ratio (W/C) was 0.4 with superplasticizer of 0.2% by weight of cement. This mix was based on several trial mixes in order to achieve the most appropriate mix to produce good workability and uniform mixing of concrete without segregation. Steel fiber reinforced concrete was obtained by adding steel fibers with volume fractions of 0.4% and 0.8% *v<sub>f</sub>* to the fresh non-fibrous concrete mix, and remixed.

## 3. Experimental Work

### 3.1. Molds Preparation

Six wooden plywood molds are designed and fabricated for casting all (6) beams. The molds are made of (700) mm length, (100) mm width and (100) mm height and their side pieces are connected by bolts which can easily removed to strip off the hardened beams after casting. All molds have been well connected, cleaned, oiled, before pouring of concrete mixture into them.

### 3.2. Mixing

In order to obtain a homogenous concrete mixture with sufficient workability a certain producer used. All batching was done by weight .The concrete was mixed using electrical mixer. The interior surface of the mixer was cleaned and moistened before placing the materials. First both coarse and fine aggregate placed and mixed for several minute in the mixer after that cement was added, The materials were mixed until a uniform color was obtained, After that half of the water quantity was added and mixed for several minutes too. The Fluidifying agent (Visco Crete -5930) quantity was split into two halves, first half was added to the remain water and moved by a sticker till homogenous mixture obtained before adding to the mixture and mixed for 5 minutes,

Finally the rest of the Fluidifying agent (Visco Crete -5930) quantity was added to the mixture and mixed for about 3 minutes. When steel fiber was added to the mix it was uniformly distributed by several nodes in the top of the mixer.

### 3.3. Casting, Compaction, and Curing

After mixing the concrete mixture poured into molds in two layers, when each layer laid; the sides of the molds was hammered by rubber driver, to shake the mix and consolidate it into the molds. Then was compacted using a table vibrator compactor in case of normal compaction for about 40 seconds for each layer During compaction air bubbles will appear on the surface as an indication of dispossessing unwanted air. After that the surface of concrete was leveled off and finished with a trowel. Then, the specimens were covered to prevent evaporation of water. After (24) hours, the specimens were stripped from the molds and cured in a water bath with 28° temperature for about one month. Since water temperature would be below the desire temperature degree heater was used in cold weather to achieve adequate curing.

## 4. Strength and Mechanical Properties of Hardened Concrete

### 4.1. Compressive strength ( $f'_{cu}$ )

The compressive strength test was carried out in Material Laboratory of Engineering faculty in Al- Mustansiriya University for both fibrous and non-fibrous concrete according to ASTM C39 [5] using a standard cubes specimens with dimensions (100 × 100 × 100)mm for length, width, height respectively. Then the specimens loaded uniaxially using the universal testing machine (ELE, Digital Elect 2000).

### 4.2. Splitting Tensile Strength ( $f_t$ )

Indirect tensile strength was carried out in Material Laboratory of Engineering faculty in Al- Mustansiriayah University on non-fibrous, and fibrous concrete specimens in accordance with ASTM-C496 [5] Using standard cylinders specimens with (100) mm diameter and (200) mm height. The test carried out by placing a cylinder specimen horizontally in the compression testing machine and load applied until failure occurred. The splitting tensile strength is calculated from the following equation:

$$\sigma_t = \frac{2 P}{\pi L D} \quad (1)$$

Where:

$\sigma_t$ : Splitting tensile strength (MPa),

P: Applied compressive load (N),

L: Length of cylinder (mm),

D: Diameter of cylinder (mm).

### 4.3. Modulus of Elasticity ( $E_c$ )

#### 4.3.1. Equation Method

Measurements of static modulus of elasticity of concrete ( $E_c$ ) is determined by obtained compressive strength of concrete and SFRC of cube specimens by conducting compressive strength test and then using the following equation [6];

$$E = 3320\sqrt{f_{cu}} + 6900 \quad (2)$$

Where;

$E$ : Elastic modulus (MPa),

$f_{cu}$ : Compressive strength (MPa).

#### 4.3.2. Ultrasonic Test Method

Portable Ultrasonic Non-destructive Digital Indicating Test (PUNDIT) is used to determine young modulus for concrete beam, cube and cylinder specimens. The device contains two transducers, one as transmitter and the other one as receiver, which used to send and receive frequency. The time that the wave takes to travel is read out and the velocity of wave transport can be calculated using the following equation; [7]

$$v = \frac{L}{t} \quad (3)$$

Where;

$v$  = Velocity of the wave, km/sec.

$L$  = Distance between transducers, mm.

$t$  = Traveling time,  $\mu$ sec.

Then following equation is used to determine young modulus for concrete; [8]

$$E = \rho v^2 \frac{(1 + \nu)(1 - 2\nu)}{(1 - \nu)} \quad (4)$$

Where;

$E$ : Elastic modulus (MPa),

$\rho$ : Density ( $\text{kg/m}^3$ ),

$\nu$ : Pulse velocity (km/s), and

$\nu$ : Poisson's ratio.

### 4.4. Flexural Strength Test

Six beam specimens were subjected to flexural strength test (Three Point Bending Test) using a hydraulically increasing universal testing machine under monotonic loads up to ultimate load with two different rate of loading, first rate of loading was (0.5

kN/sec) and the second was (1 kN/sec) at the structural laboratory of the faculty of Engineering, Al-Mustansiriya University. The tested beam specimens were simply supported at ends over an effective span length of (600) mm, and loaded with one-point loads. Vertical deflections were measured at the top surface of the concrete beam at a distance of (50) mm from the center of load applied as shown in Fig (2) by using dial gauges of (0.01) mm accuracy with (30) mm capacity.

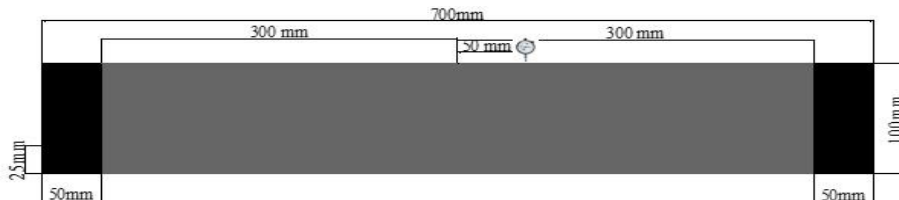


Figure 2. Digital Gage Position on Concrete Beam Surface.

#### 4.5. Strain Measurement

Uniaxial electrical resistance (foil) strain gage was the adopted method to measure the strain in all concrete beam specimens. A 60 mm of pre-wired strain gages of (120 $\Omega$ ) resistance, made in Japan for TML (TML, Tokyo Sokki Kenkyujo Co., Ltd, Japan, [www.tml.jp/e](http://www.tml.jp/e)), were used in the test. The strain gages were normally installed by the recommended adhesive (CN-E). After the contact surface was suitably prepared, strain gages position on concrete beam surface on the tension portion at a distance of 25 mm of bottom edge of the concrete beam and (0.4 L) distance from the center of load applied in flexural strength test, which (L) is the effective length of concrete beam as shown in Fig (3). The test program of strain included unique techniques used. The NIC Jaipur (NIC, Jaipur (A Sensor & Automation Company), India. [www.micsensorautomation.com](http://www.micsensorautomation.com).) multichannel data logger of DAM-XC-USB-350 series model is used to measure strain.

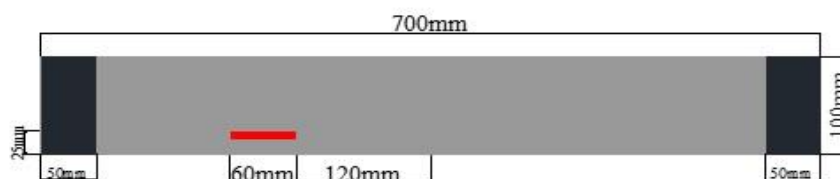


Figure 3. Strain Gage Position.

## 5. Results and Discussion

### 5.1. Compressive Strength

The compressive strength ( $f_{cu}$ ) of plain and steel fiber reinforced concrete beam specimens increase as steel fiber content increase at which factor of increasing increased from (1.09) to (1.29) for (0.4) % and (0.8) %  $V_f$  of steel fiber respectively as shown in Fig (4).

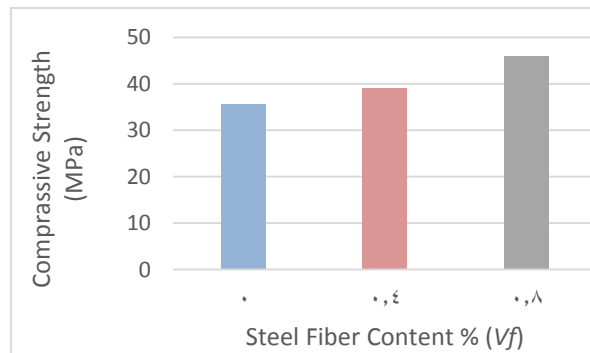


Figure 4. Compressive Strength Test Results.

### 5.2. Splitting Tensile Test

The tensile strength ( $f_t$ ) for (0.0, 0.4 and 0.8) % ( $v_f$ ) of steel fiber is obtained and the test results show that the tensile strength increase as steel fiber content increase by factor of increasing which was about (1.4) and (1.88) for (0.4) % and (0.8) % steel fiber content respectively as shown in Fig (5).

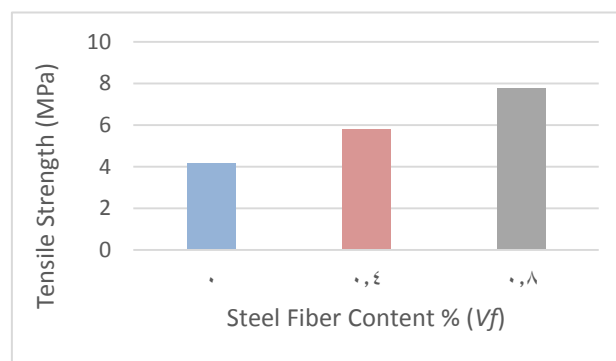


Figure 5. Tensile Strength Test Results.

### 5.3. Modulus of Elasticity

The modulus of elasticity for (0.0, 0.4 and 0.8) % ( $v_f$ ) of steel fiber is obtained and the test results show that the modulus of elasticity increase as steel fiber content increase, modulus of elasticity results along with factor of increasing are shown in Table (9).

Table 9. Modulus of Elasticity for Flexural Strength Test.

Sample	$E_c$ equation (GPa)	Factor of Increasing	$E_c$ ultrasonic (GPa)					
			Cube	Factor of Increasing	Cylinder	Factor of Increasing	Beam	Factor of Increasing
A	24.85	-	37.5	-	44.63	-	40.18	-
B	25.68	1.03	39.45	1.05	46.73	1.05	42.39	1.06
C	27.29	1.1	44.63	1.19	51.39	1.15	43.94	1.09

## 5.4. Flexural Strength Test

### 5.4.1. Load-Deflection Curves

Flexural strength test is conducted to (0.0, 0.4, 0.8) %  $V_f$  of steel fiber concrete beam specimens at (0.5) and (1) kN/sec rate of loading, the three point bending test method is used and the obtained results represented by load-deflection at which deflection is measured at (50) mm from load applied point, load-deflection curves are shown in Figs (6) and (7) for (0.5) and (1) kN/sec rate of loading respectively.

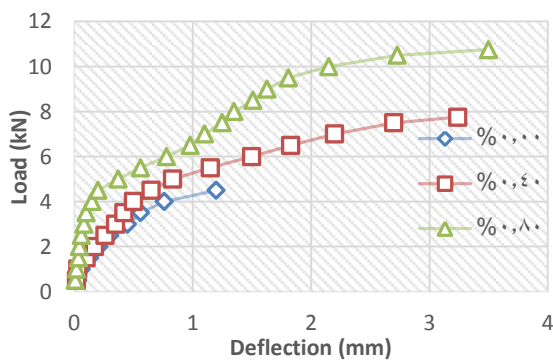


Figure 6. Load-Deflection Curves for Concrete Beam Specimens for (0.5 kN/sec) Rate of Loading.

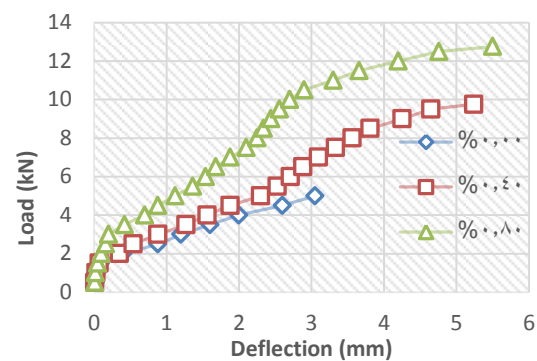


Figure 7. Load-Deflection Curves for Concrete Beam Specimens for (1) kN/sec Rate of Loading.

### 5.4.2. Stress-Strain Curves

The stress-strain relation of steel fiber reinforced concrete beam specimens are shown in Figs (8) and (9) for (0.0, 0.4 and 0.8) % steel fiber content at (0.5) and (1) kN/sec rate of loading respectively. Figures showed that as steel fiber content increase concrete become stiffer while toughness and ductility are increased. Strain values are measured on concrete beam specimen surface on tension zone at a distance of (250) mm from the bottom edge of the concrete beam and (0.4 L) that is (240) mm distance from the center of load applied of three point bending test to strain gauge edge at which (L) is the effective length of concrete beam which is (600) mm.

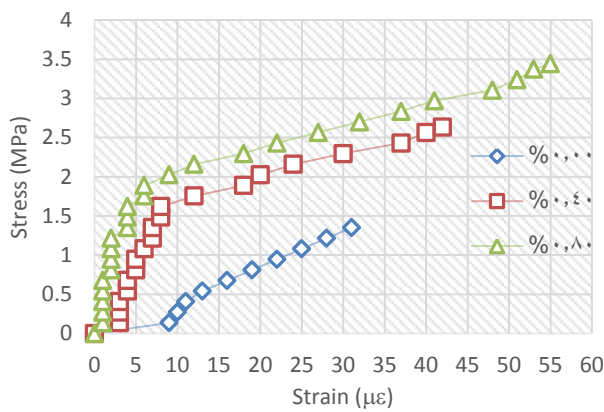


Figure 8. Stress-Strain Curves for Concrete Beam Specimens for (0.5) kN/sec Rate of Loading.

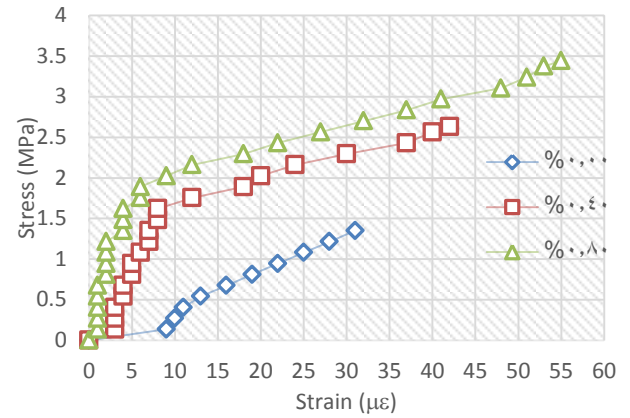


Figure 9. Stress-Strain Curves for Concrete Beam Specimens for (1) kN/sec Rate of Loading.

## 6. Analysis of Finite Element Program ABAQUS

### 6.1. Analysis Using Linear Elastic Model

For finite element analysis six beam specimens are involved for three point loading test with (0.0, 0.4 and 0.8) % (*vf*) and two rates of loading (0.5 and 1) kN/sec, to predict and simulate the behavior of concrete and SFRC pavement with inclusion of steel fiber by computing stress, strain and deflection meantime create a comparison between the experimental works and finite element analyses results. To create a new model select Part Create from the main menu bar. The part designed in this study is (Modeling space 3D-Planer deformable type) for beam, fixed pins and load applied.

The beam is drawn with (700) mm length (100) mm width and (100) mm depth, fixed pins is steel roller with (75) mm diameter and (300) mm length and the load applied steel roller with (25) mm diameter and (225) mm length. For material property of beam specimens, from (Edit Material dialog box) select (Material  $\Rightarrow$  Create) from the main menu bar, material properties is created to both concrete and steel, both material is assumed to be elastic with modulus of elasticity for concrete using Eq. (2). Material properties along with modulus of elasticity and poisson's ratio are shown in Table (10).

Table 10. The Input Data of ABAQUS Program.

Material Properties	% <i>vf</i> of Steel Fiber	Modulus of Elasticity (GPa)	Poisson's Ratio	
Concrete	Beam (A)	0.0	25.24	0.2(assumed)
	Beam (B)	0.4	26.86	0.2(assumed)
	Beam (C)	0.8	29.57	0.2 (assumed)
Steel	-	-	200 (assumed)	0.305 (assumed)

For mesh size a sequence of finite element analyses is performed with decreasing the element size to determine the appropriate and most accurate mesh size. Mesh is created for each element with  $\Rightarrow$  sizing  $\Rightarrow$  control. Approximate global size of (10) for beam, (5) for load applied roller as finer mesh leads to more accurate analysis, and (15) for fixed rollers as shown in Fig (10). Interaction for the model is created between load applied roller and beam surface at which *ABAQUS*/Standard has several contact formulations. Each formulation is based on a select of a contact discretization, a tracking approach, and assignment of “master” and “slave” roles to the contact surfaces. The assignment of “master” and “slave” roles to the contact surfaces is used to model the interaction between any two layers in partially contact.

To generate a load and boundary conditions select Create from the suitable menu in the main menu bar and choose the type of the prescribed condition that wanted to be generated. Loading condition for the model (BC1) is simulated by deflection magnitude (U2), type of boundary condition was (Displacement/Rotation) for each %  $v_f$  of steel fiber (0.0, 0.4 and 0.8) while boundary conditions for fixed rollers (BC2) and (BC3) is mechanical Initial (Symmetry, Antisymmetry, Encastre) ENCASTRE ( $U_1 = U_2 = U_3 = UR_1 = UR_2 = UR_3 = 0$ ). And surfaces of load applied roller and beam specimen were fixed (BC4) in the z direction to prevent the movement of the two element during load application, type of boundary condition is (Displacement/Rotation) and (U3) is equal to (0). The boundary condition of three point bending test *ABAQUS* model is shown in Fig (10).

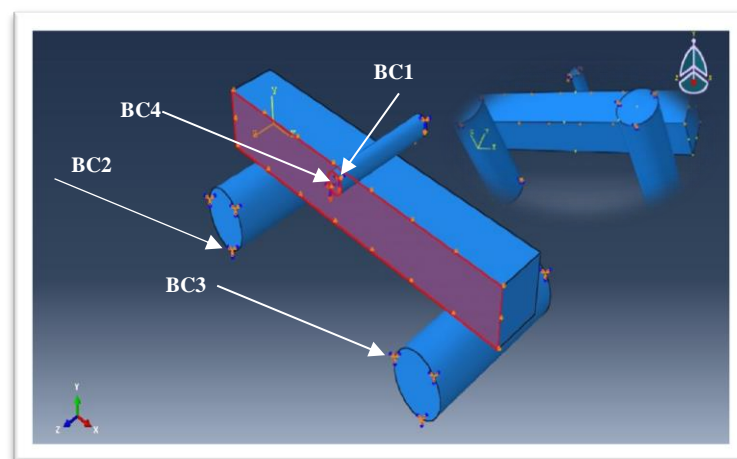


Figure 10. Boundary Conditions for the Model by *ABAQUS*.

## 6.2. Analysis and Comparison between Experimental and Numerical *ABAQUS* Results

The results of finite element program include the distribution of the stress, strain and displacements have been considered for rigid pavement. Figs. (11), (12) and (13) show the distribution of stress, strain and displacements for (0.0) %  $v_f$  beam specimen at (0.5) kN/sec rate of loading respectively. All other beam specimens' analysis are shown in appendix A.

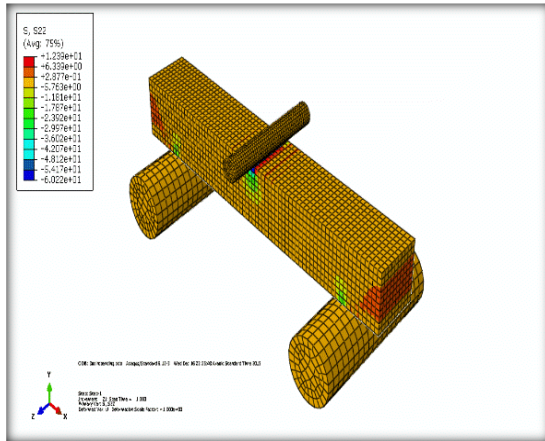


Figure 11. Distribution of Vertical Stresses for Beam with (0.0) %  $v_f$  at (0.5) kN/sec Rate of Loading.

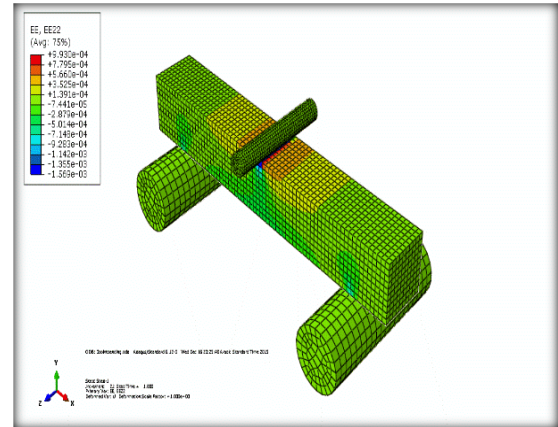


Figure 12. Distribution of Vertical Strain for Beam with (0.0) %  $v_f$  at (0.5) kN/sec Rate of Loading.

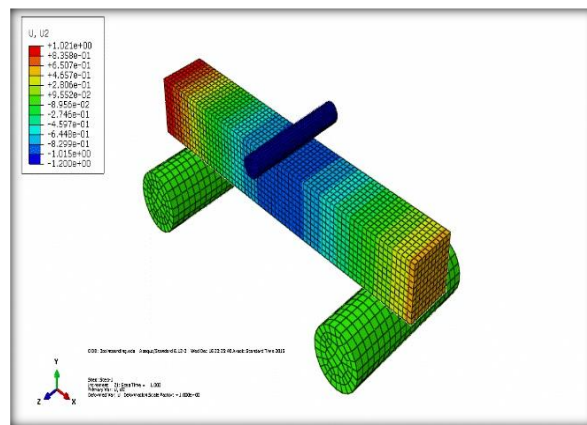


Figure 13. Distribution of Vertical Deflection for Beam with (0.0) %  $v_f$  at (0.5) kN/sec Rate of Loading.

Comparison has been carried out between experimental results and *ABAQUS* outputs for (0.0, 0.4 and 0.8) %  $v_f$  of steel fiber content at (0.5) kN/sec rate of loading at a distance of (25) mm from concrete beam edge and (0.4 L) that is (240) mm distance from the center of load applied of three point bending test. A good agreement can be seen between the experimental results and the analytical approaches as shown in Figs (14) and (15).

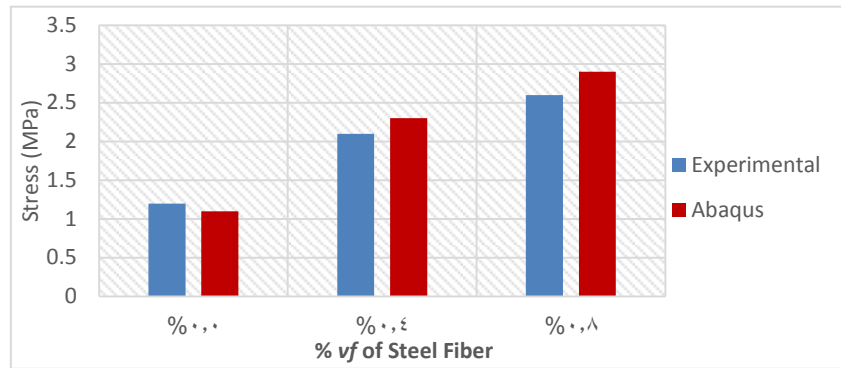


Figure 14. Comparison of Vertical Stress between Experimental and ABAQUS Results at (0.5) kN/sec Rate of Loading.

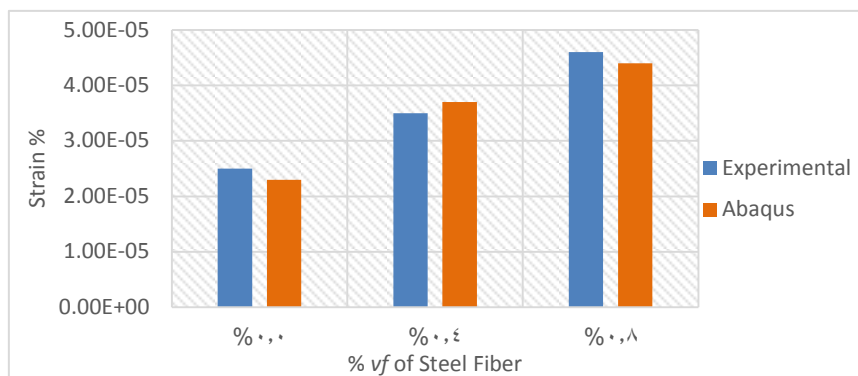


Figure 15. Comparison of Vertical Strain between Experimental and ABAQUS Results at (0.5) Rate of Loading.

Comparison has also been carried out between horizontal tensile stress and strain at bottom of concrete pavement for (0.0, 0.4, and 0.8) % vf of steel fiber content as shown in Figs (16) and (17) respectively. Which show that as steel fiber content increase in concrete, the magnitudes of stress and strain that SFRC can withstand without deterioration increase significantly.

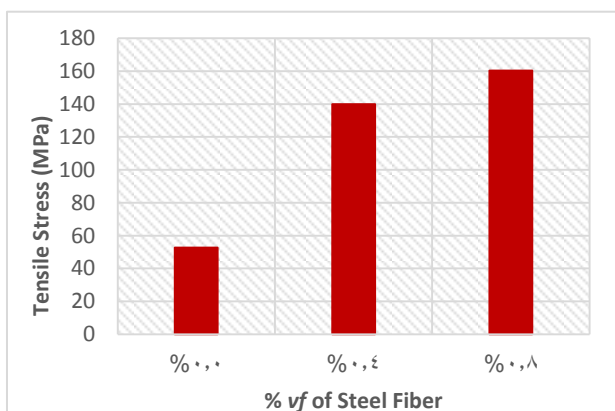


Figure 16. Comparison of Horizontal Tensile Stress of Concrete from ABAQUS Results at (0.5) kN/sec Rate of Loading.

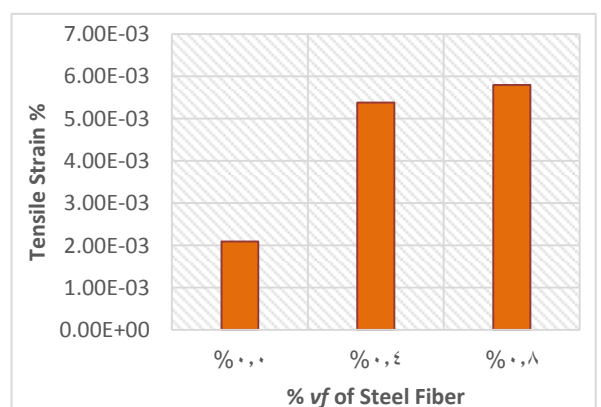


Figure 17. Comparison of Horizontal Tensile Strain of Concrete from ABAQUS Results at (0.5) kN/sec Rate of Loading.

Figs (18) and (19) show Comparison between stress and strain respectively for experimental outcomes and software outputs of (0.0, 0.4 and 0.8) % $\nu_f$  of steel fiber at (1) kN/sec rate of loading and good agreement can be seen between the experimental results and the analytical approaches.

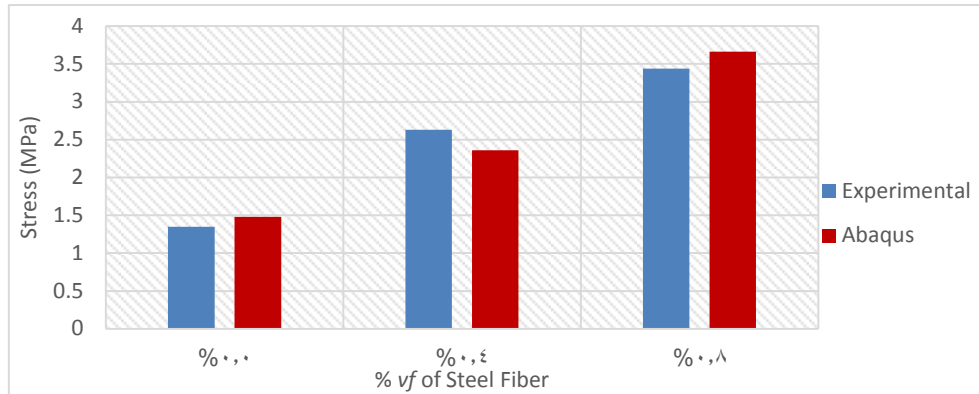


Figure 18. Comparison of Vertical Stress between Experimental and ABAQUS Results at (1) kN/sec Rate of Loading.

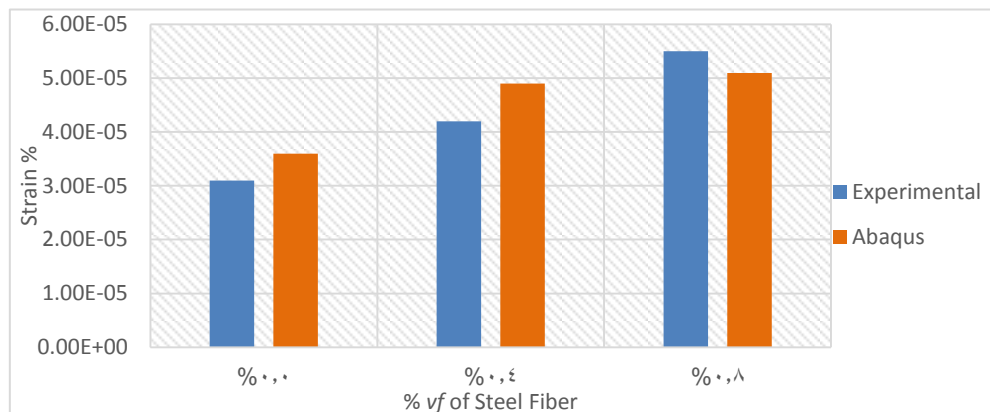


Figure 19. Comparison of Vertical Strain between Experimental and ABAQUS Results at (1) kN/sec Rate of Loading.

## 7. Conclusions

1. The experimental flexural strength test (three point bending load test) results present an expected trend of concrete behavior that, as the rate of loading increases; the flexural strength magnitude increases along with the increment of steel fiber content % ( $\nu_f$ ). Moreover, both of load at first crack ( $P_{crack}$ ) and ultimate load ( $P_u$ ) magnitudes are increased along with the increment of rate of loading from (0.5 to 1) kN/sec which approve that bridging mechanism of steel fiber works more efficiently at higher speed rates at which factor of increasing for ( $P_{crack}$ ) are (1.4), (1.67) and (1.49) for (0.0) %, (0.4) % and (0.8) %  $\nu_f$  of steel fiber respectively, while factor of increasing for ( $P_u$ ) are (1.11), (1.26) and (1.19) for (0.0), (0.4) and (0.8) %  $\nu_f$  of steel fiber respectively.
2. Due to high tensile strength of steel fiber; the SFRC become stiffer under flexural strength test which enhance the capability of SFRC to withstand higher load magnitude

- at first crack ( $P_{crack}$ ) as a result factor of increasing of ( $P_{crack}$ ) as compared to ordinary concrete was (1.2) and (1.5) for (0.4) %  $v_f$  of steel fiber content at (0.5) kN/sec rate of loading and (1.4) , (1.6) for (0.8) %  $v_f$  of steel fiber at (1.0) kN/sec rate of loading.
3. The magnitude of toughness is increased as steel fiber content increase comparing to plain concrete by (4.82) and (7.38) for (0.4 and (0.8) %  $V_f$  of steel fiber respectively at (0.5) kN/sec rate of loading. And by (3.1) and (4.83) for (0.4 and 0.8) %  $V_f$  of steel fiber respectively at (1) kN/sec rate of loading.
  4. Compressive strength, tensile strength and modulus of elasticity magnitudes are also increased along with the increment of steel fiber due to the high tensile strength and competency of steel fibers to arrest micro cracks and break the propagation of cracks until the composite ultimate stress of SFRC is extended.
  5. A good agreement can be seen between the experimental and the analytical results of numerical model developed at which finite element method may be used to simulate deflection of three-point-bending occurred in concrete beam specimens.
  6. Comparison between horizontal tensile stress and strain at bottom of concrete pavement for (0.0, 0.4, and 0.8) %  $v_f$  of steel fiber content show that as steel fiber content increase the ability of concrete pavement to withstand higher magnitudes of stress and strain without deterioration increase significantly due to high tensile strength of steel fiber.

## Abbreviations

SFRC	Steel Fiber Reinforced Concrete
FEM	Finite Element Method
PCC	Portland Cement Concrete Pavement
NCCLR	National Center for Construction Laboratories and Research
$f'_{cu}$	Compressive Strength
$f_t$	Splitting Tensile Strength
$E_c$	Modulus of Elasticity
W/C	Water Cement Ratio
$\sigma_t$	Splitting Tensile Strength
P	Applied Compressive Load
L	Length of Cylinder
D	Diameter of Cylinder
v	Velocity of the Wave, km/sec
L	Distance between Transducers, mm.
t	Traveling Time, $\mu$ sec
$\rho$	Density (kg/m <sup>3</sup> )
$\nu$	Poisson's Ratio
v	Pulse Velocity (km/s)
$V_f$	Volume Fraction of Steel Fiber
$P_{crack}$	Load at First Crack
$P_u$	Ultimate Load

## 8. References

1. ACI 544.1R-96. (2002). " *State-of-the-Art Report on Fiber Reinforced Concrete*".
2. ACI 544.3R-93. (1998). " *Guide for Specifying, Proportioning, Mixing, Placing, and Finishing Steel Fiber Reinforced Concrete*".
3. ABAQUS 6.12 " *Abaqus/CAE User's Manual*". (2011), Internet Manual. Simulia. Retrieved 10.
4. V. D. R. Kumar; S. Krishna Rao; B. Panduranga Rao.,(2013), "A Study On Properties Of Steel Fibre Reinforced Roller Compacted Concrete" International Journal of Engineering Sciences & Emerging Technologies. Volume 6, pp 221-227.
5. ASTM Designation C39-86., (1989), " *Compressive Strength of Cylindrical Concrete Specimens*" Annual Book of ASTM Standards, American Society for Testing and Materials, Philadelphia, Pennsylvania.
6. ASTM C496-79., (1979), " *Standard Method of Test for Splitting Tensile Strength of Cylindrical Concrete Specimens*", American Society for Testing and Materials.
7. Carrasquillo, R. L., Nilson, A. H., and Slate, F.O., (1981), " *Properties of High Strength Concrete Subject to Short-Term Loads*", ACI Journal, Vol. 78, No. 3, PP. 171-178.
8. Baqer Abdul Hussein Ali, (2008), " *Assessment of Concrete Compressive Strength by Ultrasonic Non-Destructive Test*", M.Sc. Thesis, Department of Civil Engineering, University of Baghdad.
9. British Standards Institution, (1988), " *Testing Concrete. Recommendations for Measurement of Velocity of Ultrasonic Pulses in Concrete*", Milton Keynes: BS188, part 203.

## Appendix – A

### 1. Analysis and Results for (0.5) kN/sec Rate of Loading

Vertical stress and strain along with deflection have been extracted from **ABAQUS** computer program at (0.5) kN/sec rate of loading as shown in Figs. (A1), (A2), and (A3) respectively for (0.4) %  $v_f$  of steel fiber.

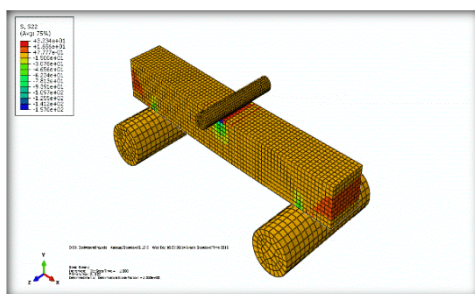


Figure A1. Distribution of Vertical Stresses for Beam with (0.4) %  $v_f$  at (0.5) kN/sec Rate of Loading.

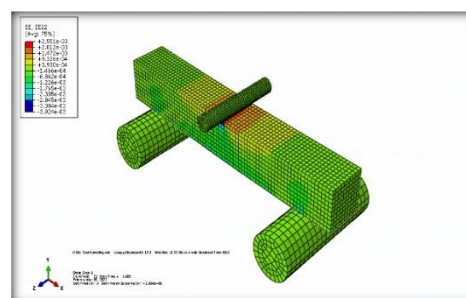


Figure A2. Distribution of Vertical Strain for Beam with (0.4) %  $v_f$  at (0.5) kN/sec Rate of Loading.

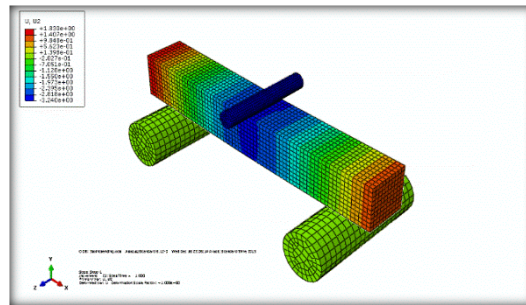


Figure A3. Distribution of Vertical Deflection for Beam with (0.4) % vf at (0.5) kN/sec Rate of Loading.

While Vertical stress and strain along with deflection have been extracted from *ABAQUS* computer program at (0.5) kN/sec rate of loading as shown in Fig. A4, A5, and A6 respectively for (0.8) % vf of steel fiber.

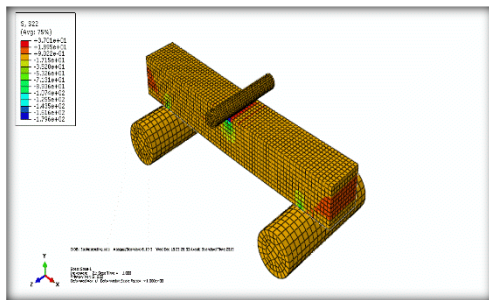


Figure A4. Distribution of Vertical Stresses for Beam with (0.8) % vf at (0.5) kN/sec Rate of Loading.

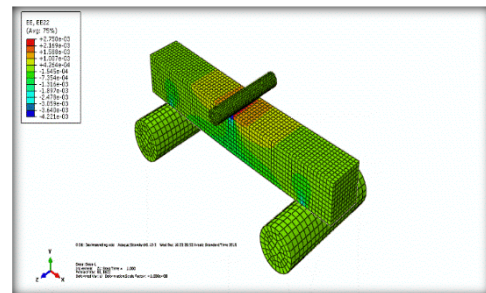


Figure A5. Distribution of Vertical Strain for Beam with (0.8) % vf at (0.5) kN/sec Rate of Loading.

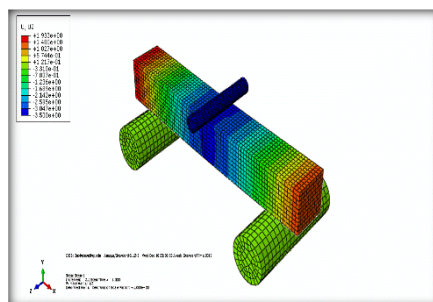


Figure A6. Distribution of Vertical Deflection for Beam with (0.8) % vf at (0.5) kN/sec Rate of Loading.

## 2. Analysis and Results for (1) kN/sec Rate of Loading

Vertical stress and strain along with deflection have been extracted from *ABAQUS* computer program at (1) kN/sec rate of loading as shown in Figs. (A7), (A8), and (A9) respectively for (0.0) % vf of steel fiber.

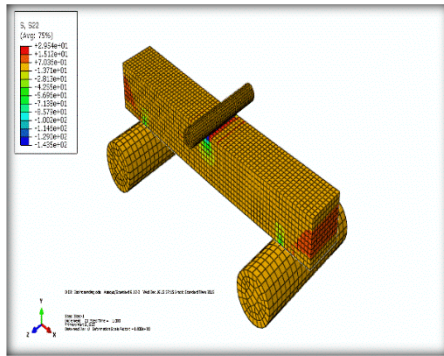


Figure A7. Distribution of Vertical Stress for Beam with (0.0) %  $v_f$  at (1) kN/sec Rate of Loading.

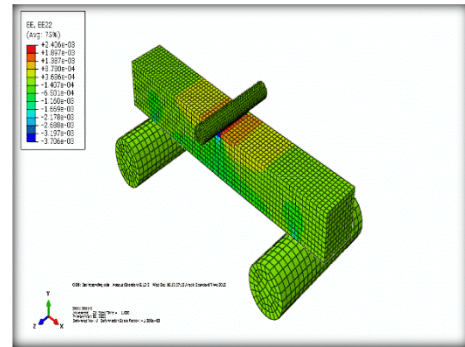


Figure A8. Distribution of Vertical Strain for Beam with (0.0) %  $v_f$  at (1) kN/sec Rate of Loading.

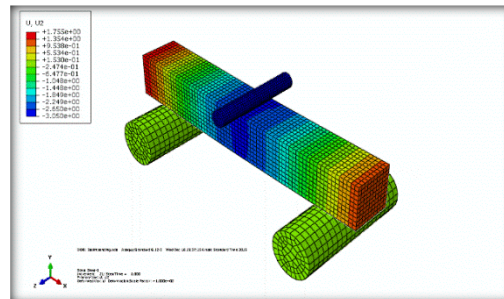


Figure A9. Distribution of Vertical Deflection for Beam with (0.0) %  $v_f$  at (1) kN/sec Rate of Loading.

While Vertical stress and strain along with deflection have been extracted from *ABAQUS* computer program at (1) kN/sec rate of loading as shown in Figs. (A10), (A11), and (A12) respectively for (0.4) %  $v_f$  of steel fiber.

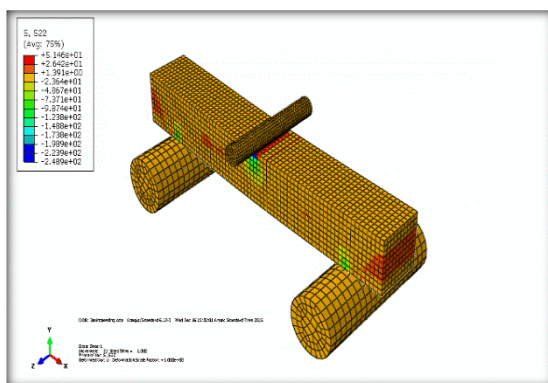


Figure A10. Distribution of Vertical Stress for Beam with (0.4) %  $v_f$  at (1) kN/sec Rate of Loading.

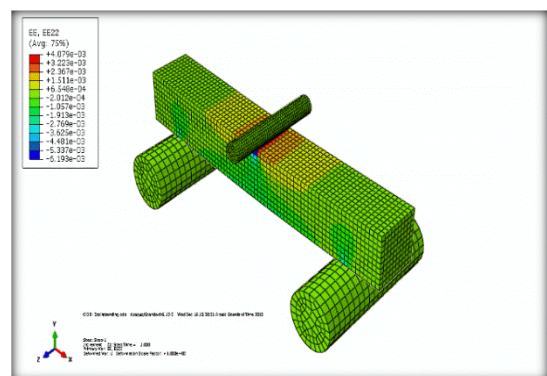


Figure A11. Distribution of Vertical Strain for Beam with (0.4) %  $v_f$  at (1) kN/sec Rate of Loading

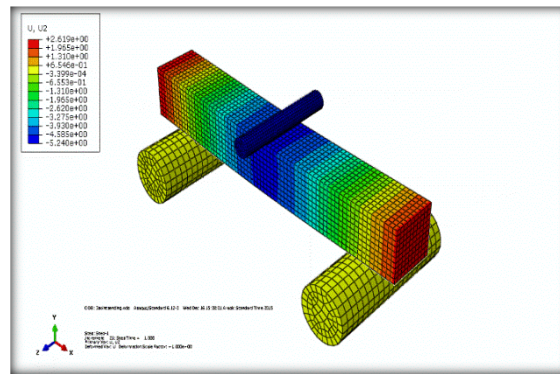


Figure A12. Distribution of Vertical Deflection for Beam with (0.4) % vf at (1) kN/sec Rate of Loading.

Finally Vertical stress and strain along with deflection have been extracted from ABAQUS computer program at (1) kN/sec rate of loading as shown in Figs. (A13), (A14), and (A15) respectively for (0.8) % vf of steel fiber.

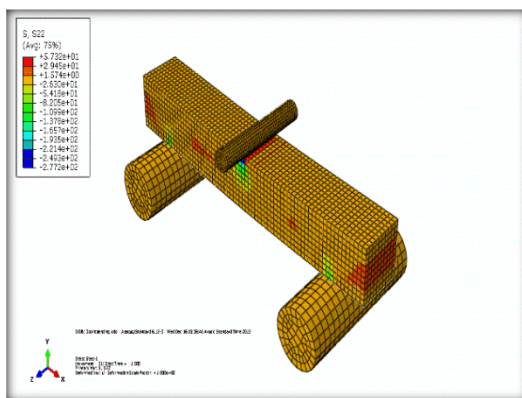


Figure A13. Distribution of Vertical Stress for Beam with (0.8) % vf at (1) kN/sec Rate of Loading.

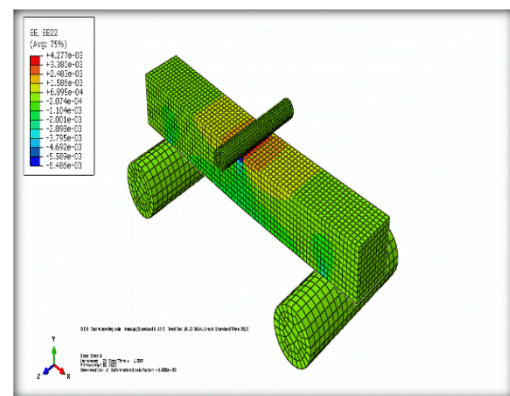


Figure A14. Distribution of Vertical Strain for Beam with (0.8) % vf at (1) kN/sec Rate of Loading.

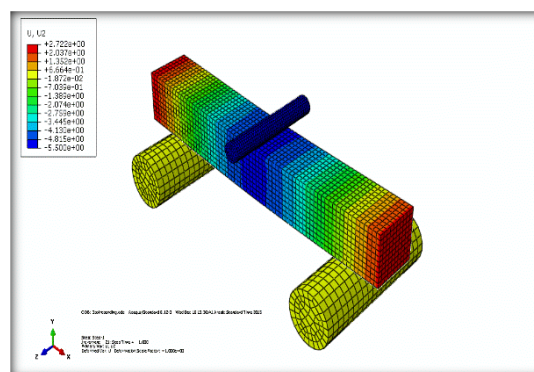


Figure A15. Distribution of Vertical Deflection for Beam with (0.8) % vf at (1) kN/sec Rate of Loading.